Materials Today • Volume xxx, Number xx • xxxx 2021 RESEARCH

ELSEVIER

RESEARCH: Original Research

Interfacing DNA hydrogels with ceramics for biofunctional architectural materials

Yehudah A. Pardo [1,†], Kenneth G. Yancey [2,†], David S. Rosenwasser [3], David M. Bassen [1], Jonathan T. Butcher [1], Jenny E. Sabin [3], Minglin Ma [2], Shogo Hamada [2,‡], Dan Luo [2,*]

[1] Meinig School of Biomedical Engineering, Cornell University, Weill Hall, 237 Tower Rd., Ithaca, NY 14853, United States
[2] Department of Biological and Environmental Engineering, Cornell University, Riley-Robb Hall, 111 Wing Dr. Ithaca, NY 14853, United States
[3] Department of Architecture, Sibley Hall, 921 University Ave., Cornell University, Ithaca, NY 14853, United States

The development of architectural components with the capabilities of biological systems could lead to the realization of biofunctional, dynamic, interactive, and self-sustaining "living" architecture. One route to interfacing biological systems with architectural materials is functionalization with biomolecules. In particular, functionalization of surfaces with DNA incorporates both informational and active properties such as the ability to produce proteins. However, direct conjugation to surfaces can degrade biomolecule activity, reduce reaction kinetics, and limit available binding sites. Integration of DNA into a hydrogel matrix that is conjugated to the surface can overcome these limitations. Here, DNA encoding genetic information is converted into a hydrogel matrix, termed Meta P-gel. The unique mechanical properties of Meta P-gel allow it to adsorb to patterned ceramic surfaces in a spatially controlled manner. Simultaneously, Meta P-gel retains the biological ability to produce proteins, achieving spatial control over protein synthesis for potential applications in living architecture. Finally, Meta P-gel-based functionalization is applied to create stable protein gradients in situ, further exemplifying its applicability beyond architecture. These experiments are a first step toward continuous and stable protein expression from spatially controlled DNA hydrogels that would enable applications in biotechnological fields such as biosensor development and screening, and more broadly, in architectural fields such as fabrication of bioactive and bio-responsive ceramics for building façade design.

Keywords: DNA hydrogels; Ceramics; Biomaterials; Architecture; Engineered living materials

Introduction

Deoxyribonucleic acid (DNA) is a central biomolecule to life due to its unique role as a genetic template. In addition, DNA has attributes such as straightforward synthesis of designed sequences [1], predictable folding behavior [2], and long-term stability [3], which make the molecule an ideal candidate for biofunctionalization of non-biological structural components. For instance, the genetic property of DNA can be harnessed to pro-

* Corresponding author.
E-mail addresses: Pardo, Y.A. (yap6@cornell.edu), Yancey, K.G. (kgy4@cornell.edu), Rosenwasser, D.S. (dsr234@cornell.edu), Bassen, D.M. (dmb457@cornell.edu), Butcher, J.T. (jtb47@cornell.edu), Sabin, J.E. (jes557@cornell.edu), Ma, M. (mm826@cornell.edu), Hamada, S. (hamada@tohoku.ac.jp), Luo, D. (dan.luo@cornell.edu).
† These authors contributed equally to this work.
‡ Current Affiliation: Department of Robotics, Tohoku University, Japan.

 https://doi.org/10.1016/j.mattod.2021.10.029

Please cite this article in press as: Y.A. Pardo et al., Materials Today (2021), https://doi.org/10.1016/j.mattod.2021.10.029

duce proteins from the surface of functionalized materials in situ [4,5]. DNA-functionalized materials have also enabled the development of novel biosensors, drug and gene delivery systems, and various diagnostic and research tools [6–9].

Recently, a concept known as Engineered Living Materials (ELM) opened up a new class of dynamic, bioactive smart materials by interfacing architectural materials with biological systems [10]. The integration of traditional architecture materials with the functionality of biological systems could ultimately lead to architectural components with unique properties such as self-promoted growth, self-healing, and the ability to interact dynamically with the environment. Although typical ELM designs aim to directly embed cells or organisms as a living component in the material [10,11], advancements in cell-free systems allow us to create bioactive materials with functionalities such as protein production, without using living cells [12,13]. This alternative, cell-free strategy permits further flexibility and controllability in design, while retaining a high level of biofunctionality. As a first realization of this concept, here we integrate ceramic tiles, a static architectural material, and genetically functional DNA, for dynamic cell-free protein production with spatial control.

One of the common approaches for developing bioactive materials is the conjugation of DNA to 2D solid substrate surfaces [7,8]. The substrate provides structural rigidity and spatial control, while the DNA provides the biological function. For example, DNA microarrays consist of spatially addressable DNA sequences directly conjugated to a 2D surface [14]. However, restricting the biofunctionalized area to two dimensions limits the total biomolecule carrying capacity [15]. Furthermore, the reaction kinetics in a densely packed monolayer are typically slower compared to those in a solution-phase reaction [16]. To overcome these challenges, DNA has been conjugated to 3D polyacrylamide hydrogel matrices, which in turn were conjugated to a solid support [8,15,17]. In a 3D hydrogel matrix the biomolecule carrying capacity was increased more than 100 fold, and due to decreased molecular density the reaction kinetics were similar to those of a homogenous solution [8,15]. A 3D format is also naturally easier to integrate into architectural components.

Our group pioneered the development of pristine DNA hydrogels in which DNA was immobilized not by conjugation to an existing hydrogel matrix, but rather by conversion of the DNA itself into its own 3D hydrogel matrix [18–21]. One of the DNA hydrogels we developed, a mechanical metamaterial termed Metagel, displayed liquid-like physical properties [19] allowing it to adsorb to absorbent surfaces such as clay [22]. By combining these unique physical properties of Metagel with the inherent biological properties of DNA materials [20,23,24], herein we report a simple and versatile method to add biological functions to solid substrates with spatial control. Specifically, a DNA hydrogel that combines the physical properties of Metagel and the biological property of protein expression was newly developed. Thus, we created a *protein-producing* Metagel, which we termed Meta P-gel. We harnessed the properties of Meta P-gel for developing a novel method to functionalize ceramic tiles with DNA. We then illustrated that our newly created hydrogel-ceramic hybrid material provides spatial control over cell-free protein production. Finally, we demonstrated the potential of this biofunctionalized material for in situ generation of stable protein gradients that will find applications in both biotechnological and architectural fields.

Materials and methods

Formation of Meta P-gel

Plasmid DNA was digested for 5 h with an appropriate nicking enzyme (0.3 U/μL, New England Biolabs) followed by an additional 3.5 h at 37 °C with Exonuclease I and III (0.2 U/μL each, NEB) to generate sscirc templates for rolling circle amplification (RCA). Any nicking enzyme can be chosen as long as it cuts only one strand of the plasmid. Nb.BsmI was used for the plasmids encoding super-folder green fluorescent protein (sfGFP) and monomeric red fluorescent protein (mRFP1). Nt.BspQI was used for the plasmid encoding *Renilla* luciferase (RL). Following digestion, the DNA was washed two times in a 30 K MWCO spin filter to remove the digested nucleotides. The RCA reaction, containing a final concentration of 10 nM template (with annealed primer), 2.5 mM each of dATP, dTTP, dGTP and dCTP, 1× phi29 reaction buffer and 0.55 U/μL of phi29 DNA polymerase (Thermofisher Scientific) was incubated at 30 °C with 900 rpm shaking. For RCA/MCA (rolling circle amplification/multi-primed chain amplification) gels [19], MCA primers (see Supplementary Methods 1.2) were added after 8 h of RCA at a final concentration of 0.055 mM each and the reaction was allowed to proceed for an additional 60 h. For RCA only gels, the reaction was allowed to proceed for a total of 68 h. Following incubation, all gels were stored at 4 °C in sealed Eppendorf tubes until needed for up to several weeks.

Pipette aspiration

Gels (~20 μL) were submerged in Phi29 polymerase buffer (33 mM Tris-acetate, 10 mM Mg-acetate, 66 mM K-acetate, 0.1% (v/v) Tween 20, 10 mM DTT) in a 100 mm petri dish. A glass capillary tube (ID 0.5 mm) was docked on the gel surface. Pressure was applied using a p-200 pipette calibrated with a custom manometer, connected to the glass capillary via buffer-filled tubing. A pocket of air was left in the capillary tube in order to aspirate only the material being tested. The lowest pressure that ensured stable contact with the micropipette was taken as zero. Pressure loads were incremented uniformly, and the aspirated length was observed at each increment using a Zeiss Discovery v20 stereomicroscope and measured using calibrated images in NIH ImageJ. An experimental stretch ratio, λ, was defined by normalizing the aspirated length (L) to the pipette radius (r_p) as previously described [25].

Cell free protein synthesis and protein detection

CFPS was performed based on the TXTL 2.0 system described by the Noireaux group [26–28]. However, cells were lysed with a high-pressure homogenizer at 15,000 psi, the lysate was pelleted at 20,000 × *g*, and no DTT was added to the S30 A or S30 B buffers. Purified T7 RNA polymerase (Promega) was added to each CFPS reaction at a final concentration of 2.667 U/μL. The reaction was typically performed at a 15 μL volume in a 96-well half-area plate with shaking at 29 °C. To prevent evaporation during the reaction, the plate lid was tightly sealed with tape

Please cite this article in press as: Y.A. Pardo et al., Materials Today (2021), https://doi.org/10.1016/j.mattod.2021.10.029

and the wells surrounding the reaction were filled with water to provide a humidity source.

Quantitative measurements of sfGFP and mRFP1 production were performed with a fluorescent plate reader. sfGFP was detected at an excitation of 475 nm and an emission of 508 nm. mRFP1 was detected at an excitation of 555 nm and an emission of 605 nm. *Renilla* luciferase (RL) was detected via a commercial *Renilla* luciferase assay kit (Promega).

Freeze casting

Fully formed Meta P-gels were sandwiched between a PDMS mold and a glass slide and compressed by a 500 g weight pre-cooled to −80 °C. Molds for preparing micro pads were cast from master molds formed via photolithography as described previously [29]. These consisted of 10 × 10 arrays of pads, each 1 mm × 1 mm with varying thicknesses (20 μm or 100 μm). Molds for forming larger shapes such as triangles (3.4 mm side length, 2 mm thick) and circles (1.262 mm radius, 2 mm thick) were cast from PDMS off custom 3D-printed templates. The entire complex of PDMS mold, Meta P-gel, glass slide, and weight was frozen at −80 °C for at least 10 min. Hydrogel pads were separated with a razor blade on dry ice before thawing and then either scraped into a collection tube while still frozen or washed off the slide after thawing.

Functionalization of ceramic surfaces

Formation of patterned ceramic tiles

A Form2 3D printer (Formlabs) was employed to print a silica-based ceramic resin (Ceramic Resin 1L, Formlabs) into the desired shape. Excess resin was removed from the 3D printed parts in a bath of 91% isopropyl alcohol for 30 min. The parts were bisque-fired to cone 06 (~1000 °C). This process burned off the photopolymer resin and sintered the mineral materials into a durable, yet highly porous ceramic material. The tile was coated with Opulence 346 Gloss White glaze (Mid-South Ceramic Supply) and allowed to fully dry at room temperature. The excess glaze was removed with a sharp blade to expose the raised pattern beneath. Finally, the tiles were fired a second time at cone 4 (~1180 °C) to vitrify the glaze.

Functionalization of ceramic tiles with Meta P-gel

1 mm × 1 mm × 100 μm Meta P-gel pads were washed into a collection tube with 3 × 100 μL of DEPC-treated water. The pads were equilibrated at room temperature for 30 min with a 10× volume of the same mixture of salts (magnesium glutamate and potassium glutamate) and amino acids used in the CFPS reaction. Pads were pelleted at 14.1 k × g, resuspended in CFPS solution without rNTPs at a 1x final concentration, and incubated for 18 hours at 4 °C. The pads were then scattered across the ceramic surface, allowed to adsorb for 5 min, and any excess hydrogel pads were removed by inverting the ceramic tile and centrifuging at 100 × *g* for 5 min. In the case of the dual protein gradients, a custom device was used to slowly bring an inverted slide with hanging droplets of pads in contact with the dumbbell-patterned surfaces. This ensured that the two pad types (each coding for a separate protein) contacted the ceramic surface simultaneously. To initiate CFPS, the surfaces were incubated with 1× rNTPs (2× rNTPs for gradients) for 5 min at room temperature and then centrifuged again at 100 × *g* for 5 min to remove excess solution. The surfaces were incubated at room temperature to enable imaging during protein expression. Multiple image tiles covering a single ceramic surface were stitched together using the Stitching plugin [30] in Fiji (NIH ImageJ).

Results and discussion

Meta P-gel is a hydrogel network composed entirely of DNA and prepared via a combination of enzymatic amplification processes using Phi29 DNA polymerase. Specifically, rolling circle amplification (RCA) and multi-primed chain amplification (MCA) were employed to amplify a single-stranded circular (sscirc) DNA template [19]. This process produced a mixture of extremely long single-stranded and double-stranded DNA (up to ~4 × 10^5 bases, see supplementary Fig. S1 and Supplementary Discussion 2.1) cross-linked by physical entanglement and hydrogen bonding. In contrast to the original Metagel, which used a circularized synthetic template, here we converted super-coiled plasmid DNA (double-stranded, circular DNA) into an sscirc template that could be amplified via RCA (Fig. 1a, supplementary Fig. S1, see Materials and Methods 2.1).

Having successfully formed Meta P-gel, we first characterized its mechanical properties to determine if it retained the unique abilities of Metagel. Due to the low volume (10–20 μL) of the Meta P-gels developed in this study we applied pipette aspiration, a technique shown to be comparable to bulk methods of mechanical characterization of biomaterials [31], yet better suited to low-volume materials, to quantify Meta P-gel's stretch response. Meta P-gel exhibited a nonlinear stretch response, confirming that it was a solid material (Fig. 1b, supplementary Fig. S2, Supplementary Discussion 2.2). Nevertheless, in air Meta P-gel exhibited the liquid-like property of assuming the shape of its container (for example, a triangle or circle-shaped mold, Fig. 1c). This ability was an important factor in enabling Meta P-gel to coat and ultimately adsorb to solid surfaces (Fig. 3) Furthermore, when replaced in an aqueous environment, Meta P-gel remembered and returned to its original geometry even after losing its form in air (Fig. 1d, supplementary video). A previous study of Metagel suggested that these properties are due to the interplay between the modulus of the material, its elasticity, and gravity and surface tension forces [32].

Surprisingly, we discovered that freezing Meta P-gel reprogrammed its remembered shape. Even after thawing and losing its shape in air, Meta P-gel would remember and return to the shape of the mold in which it was frozen rather than the geometry in which it was originally formed (supplementary Fig. S3A, S3B). Presumably, this phenomenon is caused by reorganization of the DNA matrix similar to the reorganization of the polymer matrices that has been observed in other types of hydrogels following freezing [33,34]. This property allowed us to develop a freeze-casting methodology to control precisely the shape and volume of Meta P-gel after its formation (see Materials and Methods 2.4, supplementary Fig. S3C, S3D). We utilized this method to convert 10 μL hydrogels into ~100 micro-pads (each with dimensions 1 mm × 1 mm × 100 μm) as a preparation step for adsorbing the DNA hydrogels onto solid substrates. In this way, we increased the surface area to volume ratio of the hydro-

Please cite this article in press as: Y.A. Pardo et al., Materials Today (2021), https://doi.org/10.1016/j.mattod.2021.10.029

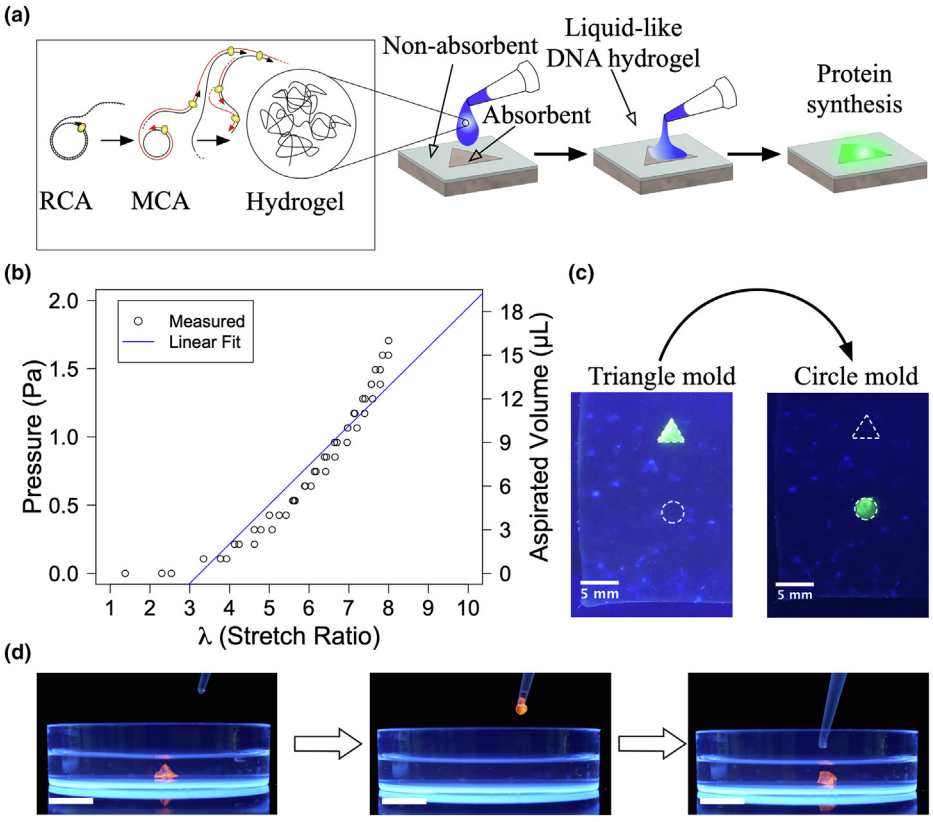

FIGURE 1

Formation and physical properties of a hydrogel meta material (Meta P-gel). (a) Scheme of process for functionalizing surfaces with Meta P-gel. After forming the gel via rolling circle amplification (RCA) and multi-primed chain amplification (MCA), it was spread on an absorbent surface allowing it to adsorb without chemical attachment. Proteins could be produced in situ by translating the DNA contained in the Meta P-gel matrix. (b) Pipette aspiration measurements showed that the stretch response was nonlinear, indicative of a solid material. $\lambda = (L + r_p)/r_p$, L = stretch distance, r_p = pipette radius. The double *y*-axis coordinates show both the net aspirated volume as well as the equivalent vacuum pressure. (c) Meta P-gel (stained with SYBR green I) acted like a liquid in air, taking on the shape of its container. When placed in a PDMS mold in the shape of a triangle, the hydrogel takes on a triangular appearance. When placed in mold in the shape of a circle, the hydrogel becomes round. The edges of the transparent molds are outlined in white for clarity. (d) Meta P-gel lost its form in air, but it would remember and return to its original geometry (triangular prism) when returned to an aqueous environment. Bars = 1 cm unless otherwise indicated.

gel, improving reaction kinetics during protein expression (see supplementary Fig. S5) and spatial resolution for protein patterning applications.

Next, we evaluated the protein expressing capability of Meta P-gel via cell-free protein synthesis (CFPS) in a standard test tube format. To demonstrate that our approach was not limited to a single protein, we synthesized two different types of hydrogel: one generated from a plasmid encoding super-folder green fluorescent protein (sfGFP) and one from a plasmid encoding *Renilla* luciferase (RL). These protein products were chosen for ease of detection and quantification; however, the same process could theoretically be applied to express any protein that is possible to produce in a cell-free fashion. Comparison to a no-gene control confirmed that both types of Meta P-gel were able to produce their respective proteins (Fig. 2a and b). In addition, we compared the yield from the Meta P-gel samples to a solution phase system (SPS) control (i.e., unamplified supercoiled plasmid in solution). We added an amount of plasmid (0.667 nM) to each SPS sample equivalent to the number of sscirc templates present in each Meta P-gel sample (10 Meta P-gel pads of 1 mm × 1 mm × 100 μm each; equivalent to 0.667 nM final concentration of template in a 15 μL reaction). If the only genes expressed in the Meta P-gel samples were those in the sscirc templates themselves, the yield from the Meta P-gel would be expected to be similar to the SPS samples. However, the measured yield from the Meta P-gel was significantly higher (up to 50-fold higher) than the SPS controls (Fig. 2a and b). This fold increase in yield is comparable to the fold difference in DNA mass between the SPS and Meta P-gel samples (~93 fold for sfGFP gels and ~53 fold for RL gels, see supplementary Fig. S1). Combined, these observations suggested that the linear DNA produced by RCA/MCA amplification served a genetic as well as a structural role in Meta P-gel.

In order to be applicable as a material for biofunctionalization, it is important that the DNA hydrogel is reusable as a genetic template for protein expression. For instance, hydrogel-based genetic templates could enable the development of continuous CFPS systems for large-scale protein production, in which the hydrogels are retained in a reactor while exchanging fresh lysate solution. The stability and reusability of Meta P-gel is also extremely important if used as an architecture material. As an illustration of this property, we reused the same ~60 Meta P-

Please cite this article in press as: Y.A. Pardo et al., Materials Today (2021), https://doi.org/10.1016/j.mattod.2021.10.029

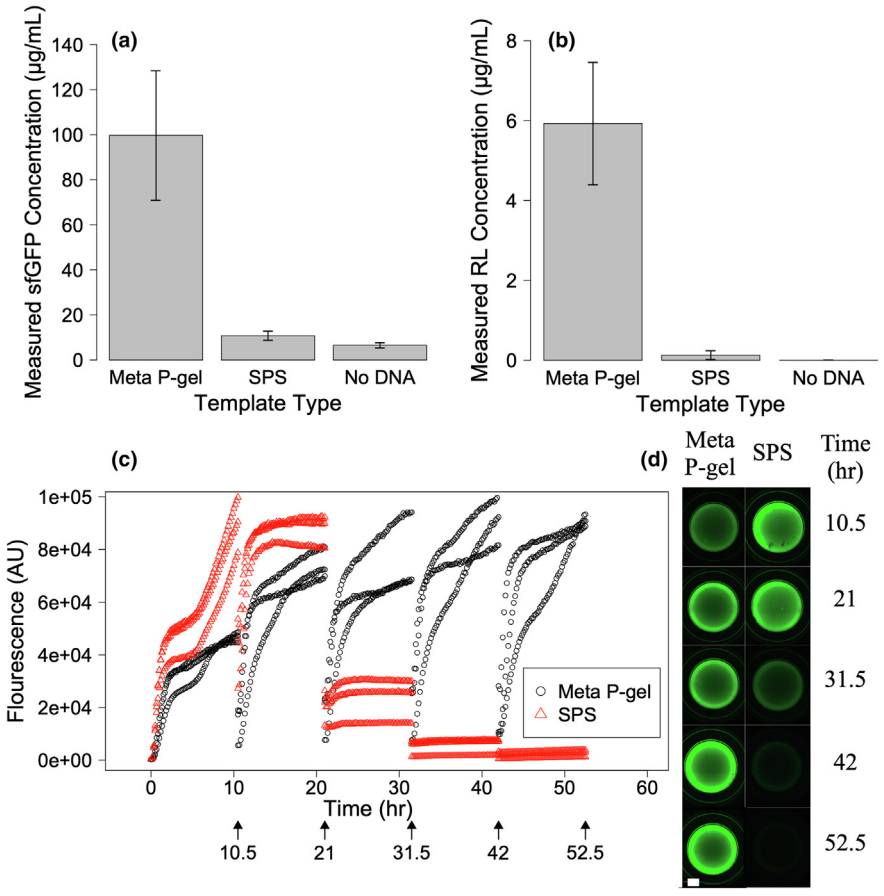

FIGURE 2

The protein expressing property of Meta P-gel. (a) Comparison of expression yield of super-folder GFP (sfGFP) of Meta P-gel to a solution phase system (SPS), i.e. unamplified super-coiled plasmid DNA (0.667 nM), and a no-gene control after overnight incubation (~15 h). (b) Comparison of expression yield of *Renilla* Luciferase (RL) of Meta P-gel to an SPS and no-gene control. (c) The fluorescence of cell-free synthesized sfGFP was measured over time from Meta P-gel and SPS samples in a 96-well plate. After 10.5 hours, the supernatant was exchanged for fresh cell-free lysate without adding additional DNA. Meta P-gel remained in the well, producing a consistent yield of sfGFP, while the plasmid in the SPS control was washed away. (d) Fluorescent images of the wells at the completion of each round of cell-free protein synthesis (indicated timepoints). Bar = 1 mm.

gel pads (1 mm × 1 mm × 20 μm each; equivalent to ~0.8 nM sscirc template in a 15 μL reaction) at least five times without diminishing the protein yield (Fig. 2c and d, supplementary Fig. S4). After each round of protein expression, we aspirated the lysate solution, leaving the Meta P-gel pads in place, and then added fresh lysate. By contrast, in an SPS control the DNA template could not be physically separated from solution. Therefore, as we exchanged the lysate solution after each round of protein synthesis, the residual plasmid was increasingly diluted, degrading protein yield (Fig. 2c and d, supplementary Fig. S5). To ensure that the SPS samples produced a high yield of protein initially, we started with an excess amount of plasmid (50 nM) instead of matching the sscirc template concentration in the pads (≃0.8 nM).

We patterned Meta P-gel on 1:1 scale 3D printed high-fire porcelain ceramic tiles that we developed for architectural applications [35] as a first realization of protein expressing architectural building-blocks. Ceramics are versatile, durable, and biocompatible materials, making them well-suited for biofunctionalization [35]. Since the ceramic tiles were highly absorbent, aqueous solutions were rapidly drawn into the body of the tile through capillary action. We hypothesize that the liquid-like property of Meta P-gel enabled it to be drawn into the surface pores of the tile based on a similar mechanism and attach strongly without the need for covalent interactions.

After splitting Meta P-gel into 1 mm × 1 mm × 20 μm pads, we added it to predefined regions of a 5.3 cm × 5.3 cm ceramic tile (Fig. 3a). Even using commercially available reagents, including commercially prepared phi29 DNA polymerase (the most expensive component), we estimate that the cost of the Meta P-gel used to functionalize this tile was less than 10 cents (see Supplementary Discussion 2.3). This inherent low cost is in contrast to the previous protein-producing DNA hydrogel, P-gel. Combined with recent developments in large scale DNA hydrogel production [24] the affordability of Meta P-gel is promising for future scaling of our process to an appropriate level for architectural applications.

To automate the patterning process, we glazed ceramic tiles (see Materials and Methods 2.5.1) to seal the surface pores in certain regions while leaving other regions exposed (Fig. 3b and c). Although both the exposed (unglazed) regions and the chosen glaze (White Opulence 346) were hydrophilic [35], Meta P-gel

Please cite this article in press as: Y.A. Pardo et al., Materials Today (2021), https://doi.org/10.1016/j.mattod.2021.10.029

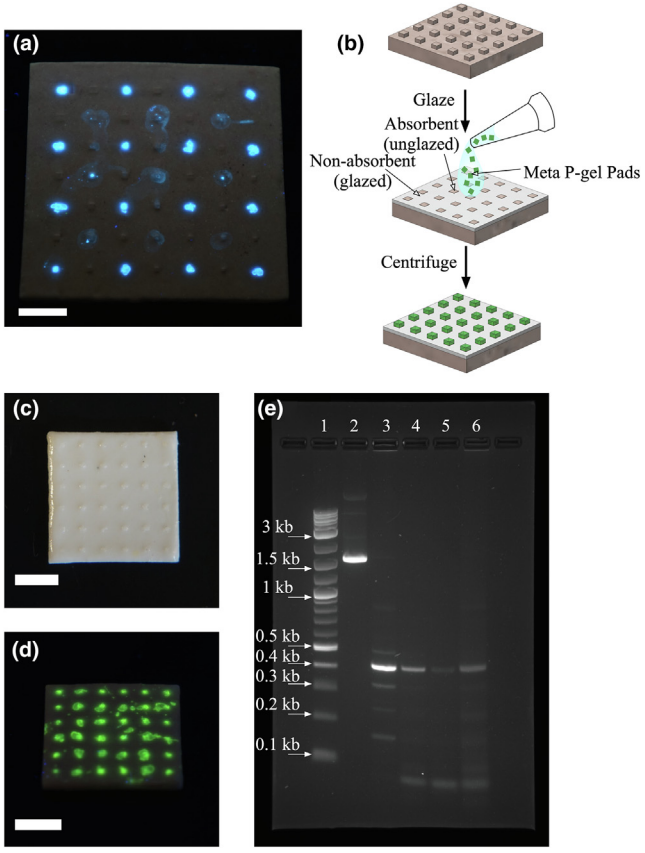

FIGURE 3

Integration of Meta P-gel with 3D printed ceramic tiles. (a) Adding Meta P-gel pads (Hoechst 33342-stained) to defined regions enabled low-cost coverage of a 3D-printed architectural tile. Bar = 1 cm. (b) The patterning process can be automated by glazing tiles to seal the surface pores and ensure that Meta P-gel pads only adsorbed to certain regions. (c) A glazed ceramic tile with an array pattern. Bar = 5 mm. (d) SYBR green I-stained Meta P-gel pads patterned in an ordered array on a ceramic tile. Bar = 5 mm. (e) The DNA sequence in the patterned Meta P-gel could be read in situ by Recombinase Polymerase Amplification (RPA). Lane 1: ladder, Lane 2: Unamplified plasmid DNA, Lane 3: Positive control RPA reaction with plasmid DNA, Lane 4–6 Triplicates of RPA from Meta P-gel patterned on a ceramic tile.

pads remained attached only to the unglazed regions after low-speed centrifugation (Fig. 3b and d). This supported our hypothesis that the attachment of Meta P-gel to the unglazed ceramic was at least partially dependent on capillary forces drawing the liquid-like hydrogel into the absorbent, unglazed tile and not strictly the surface chemistry. Even after attaching to the ceramic substrate, the genetic information encoded in the Meta P-gel matrix was still readable. As an illustration of this readability, we successfully amplified a 422 bp segment of the sfGFP gene in situ from patterned ceramic surfaces via Recombinase Polymerase Amplification (RPA) (Fig. 3e, Supplementary Methods 1.3).

To gain spatial control over protein synthesis in addition to Meta P-gel, the Meta P-gel pads were loaded with lysate prior to patterning on the ceramic surface. rNTPs were withheld from the lysate until after the pattern was formed, preventing premature transcription initiation. As a demonstration of the degree of spatial control over protein production, we scattered pads soaked in lysate across ceramic discs patterned with varied shapes (figure 8, pentagon, triangle) (Fig. 4a–c). We observed that protein synthesis (as measured by sfGFP fluorescence) was restricted to the unglazed region of the ceramic (Fig. 4a–c). To ensure that this spatial control was a unique property of the hydrogel–ceramic system, we covered similar ceramic discs with lysate droplets containing free plasmid (10 nM) rather than Meta P-gel pads. We observed that the CFPS solution was rapidly absorbed into the ceramic, and even after 4 h of incubation, no fluorescence was observed (Supplementary Fig. S6). This suggested that Meta P-gel was able to hold the lysate solution on the surface of the ceramic and maintain its functionality.

In addition to providing control over the spatial positioning of Meta P-gel pads, this ceramic-based patterning method allowed the amount of DNA hydrogel (and correspondingly, the amount of synthesized protein) per unit area to be controlled as well. This property is potentially important for controlling the sensitivity of the bioactive material to environmental conditions and the strength of its response [36]. To create a gradient of Meta P-gel density on the ceramic surface, we applied a droplet of suspended Meta P-gel pads to each end of a "dumbbell" shaped pattern (supplementary Fig. S7). As the lysate solution in which the pads were suspended was absorbed by the ceramic, the capillary force drew the pads down the length of the dumbbell. As soon as a given pad came in direct contact with ceramic, it rapidly adsorbed. Thus, as the distance from the original droplet increased, the pads available for attachment were depleted, resulting in a gradient of DNA hydrogel. After triggering protein

Please cite this article in press as: Y.A. Pardo et al., Materials Today (2021), https://doi.org/10.1016/j.mattod.2021.10.029

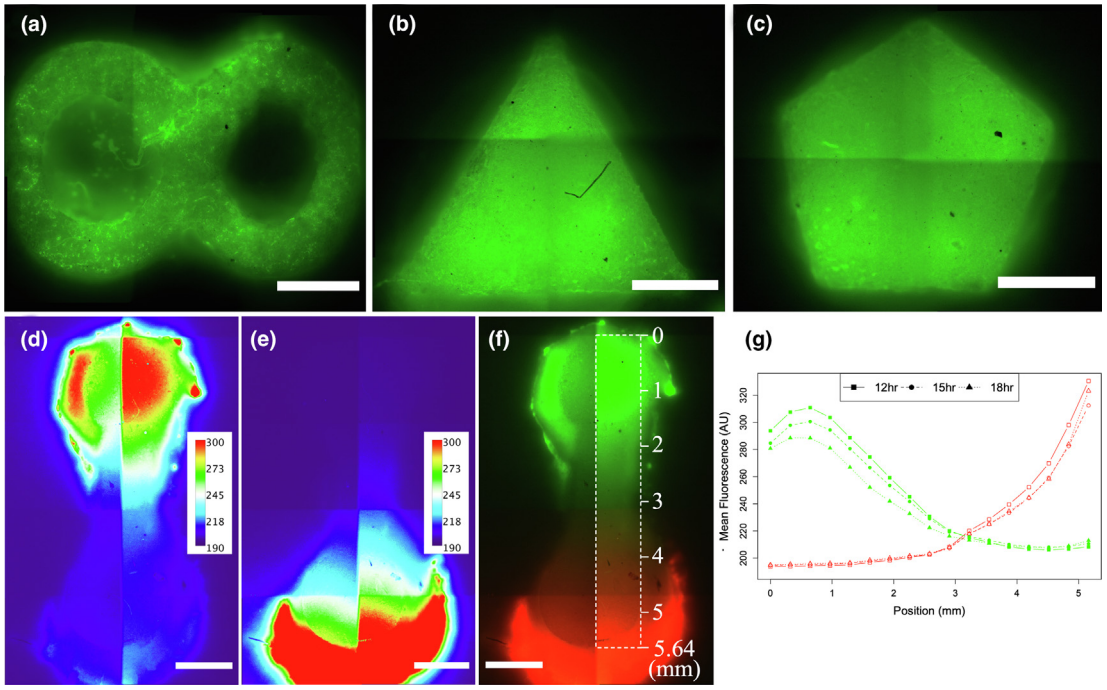

FIGURE 4

Protein expression from ceramic surfaces functionalized with Meta P-gel. Note that each image consists of multiple frames stitched together to cover the entirety of the ceramic pattern. (a–c) Fluorescent images show spatial control over expression of sfGFP. Unstained Meta P-gel pads were scattered over ceramic surfaces patterned in a figure 8 (a), triangle (b), or pentagon (c). (d–f) A dual gradient of sfGFP and mRFP1 was generated on a ceramic surface patterned with a dumbbell shape. Bars = 1 mm. Heat maps of the fluorescent intensity of the green channel (d) and red channel (e) visually illustrate the presence of a gradient of protein concentration from the edge of each dumbbell toward the center. A pseudo-colored image combining both channels shows the overall pattern of both sfGFP and mRFP1 production (f). (g) The fluorescence intensity of the green and red channels was measured within the region of the dumbbell outlined in white in panel f. Regardless of the time at which the surface was measured (12 h = square, 15 h = circle, 18 h = triangle) the gradient remained stable. Closed symbols = green channel, open symbols = red channel. Bars = 1 mm.

synthesis, a corresponding gradient of synthesized protein was established (Fig. 4d-g). We simultaneously added pads encoding sfGFP to one end of the dumbbell and pads encoding monomeric red fluorescent protein (mRFP1) to the other end, generating a dual gradient of two proteins on the same ceramic surface. To confirm that the observed gradient was stable and would not dissipate over time, we imaged the same surface after 12 hours, 15 hours, and 18 hours of protein expression (supplementary Fig. S8). A minimum time of 12 hours was chosen due to the time required for translation and maturation of the mRFP1 protein. Quantitative measurements of the fluorescent signal as a function of distance along the length of the dumbbell illustrated that the gradient had not changed over this six-hour period (Fig. 4g). The consistency of the fluorescence signal over time showed that the gradient resulted from the spatial distribution of the Meta P-gel pads rather than transient differences in expression yield across the surface.

Conclusion

In conclusion, we developed a novel route to create cell-free bioactive materials by integrating protein-producing DNA hydrogels and 3D-printed full-scale architectural ceramic tiles. The newly developed DNA hydrogel (Meta P-gel) combined the physical properties of Metagel with an ability to produce proteins in a cell-free fashion. The biofunctionality of Meta P-gel was demonstrated by creating a DNA-ceramic hybrid material with the capability to produce proteins in a spatially controlled manner. Compared to other approaches for biofunctionalization, our method is more facile since no chemical modification is necessary. More importantly, since the protein products are encapsulated in a hydrogel rather than directly bound to a surface, our method is less likely to disrupt protein activity. We illustrated the practical utility of our method for creating cell-free bioactive materials by demonstrating the reusability of the hydrogel for protein synthesis, the functionalization of ceramic tiles at an architecturally relevant scale, assembly into various patterns, and control over both the spatial patterning and concentration of the synthesized protein. Furthermore, our estimations suggested that our approach would be affordable when scaled beyond tiles.

The protein-producing ceramic tiles we developed represent a first step toward dynamic bioresponsive architectural materials. Our approach enables the rapid patterning of 3D-printed tiles at architecturally relevant scales without a need for individual pad manipulation. Furthermore, incorporating inducible promoters or aptamers in the DNA sequence could allow biosensing functionality to be implemented by triggering CFPS in the presence of an analyte of interest [37]. Integrating the biosensing and protein-producing functionality into a single tile could lead to adaptive architecture with an integrated sentinel system. In the presence of a specific trigger the material could produce enzymes

Please cite this article in press as: Y.A. Pardo et al., Materials Today (2021), https://doi.org/10.1016/j.mattod.2021.10.029

to remove or neutralize toxins, achieving dynamic sense-and-respond biofunctionality.

In addition, Meta P-gel functionalized ceramics have potential applications beyond architecture. For example, molecular gradients are directly applicable to the development of biosensors since they enable multiple concentrations to be simultaneously compared, and the sensitivity of biosensors to be tuned [38,39]. Furthermore, gradients generated from Meta P-gel-functionalized ceramic tiles share the advantages of immobilized gradients in that the protein gradient is stable once formed without requiring additional inputs [38]. At the same time, the proteins remain soluble within the DNA hydrogel matrix, reducing the likelihood that the immobilization process will inhibit molecular or cellular interactions with the gradient or deactivate sensitive proteins [40]. These properties of Meta P-gel functionalized ceramics open up new approaches toward bioengineering and biomedical applications such as drug screening, biosensors, protein patterning, detection, and diagnostics.

CRediT authorship contribution statement

Yehudah A. Pardo: Conceptualization, Methodology, Formal analysis, Investigation, Writing – original draft, Writing – review & editing, Visualization, Funding acquisition. **Kenneth G. Yancey:** Conceptualization, Methodology, Investigation, Funding acquisition. **David S. Rosenwasser:** Methodology, Investigation, Writing – review & editing. **David M. Bassen:** Methodology, Investigation, Writing – review & editing. **Jonathan T. Butcher:** Supervision. **Jenny E. Sabin:** Resources, Writing – review & editing, Supervision. **Minglin Ma:** Supervision, Funding acquisition. **Shogo Hamada:** Conceptualization, Writing – review & editing, Visualization, Supervision, Funding acquisition. **Dan Luo:** Writing – review & editing, Supervision, Project administration, Funding acquisition.

Declaration of Competing Interest

The authors declare that they have no known competing financial interests or personal relationships that could have appeared to influence the work reported in this paper.

Acknowledgements

We thank the Jewett and DeLisa labs for providing the sfGFP plasmid and the DeLisa lab for providing access to their high-pressure homogenizer. This work was supported by grants from the directorate for Engineering NSF [CBET-1530522 and CBET-1844310]. Y.P. and K.Y. contributed equally to this work.

Data availability

The raw data required to reproduce these findings are available from the corresponding author upon request. The processed data required to reproduce these findings are available from the corresponding author upon request.

Appendix A. Supplementary data

Supplementary data to this article can be found online at https://doi.org/10.1016/j.mattod.2021.10.029.

References

[1] M.H. Caruthers, Science 230 (1985) 281–285.
[2] N.C. Seeman, H.F. Sleiman, Nat. Rev. Mater. 3 (2017) 17068.
[3] M. Pruvost et al., Proc. Natl. Acad. Sci. 104 (2007) 739–744.
[4] D. Yang et al., Sci. Rep. 3 (2013) 3165.
[5] L.E. Contreras-Llano, C. Tan, Synth. Biol. 3 (2018) 1–13.
[6] D.M. Salvay, M. Zelivyanskaya, L.D. Shea, Gene Ther. 17 (2010) 1134–1141.
[7] J. Wang, Nucleic Acids Res. 28 (2000) 3011–3016.
[8] G. Yershov et al., Proc. Natl. Acad. Sci. U. S. A. 93 (1996) 4913–4918.
[9] J.S. Kahn et al., Adv. Mater. 29 (2017) 1–6.
[10] P.Q. Nguyen et al., Adv. Mater. 30 (2018) 1704847.
[11] K. Perini, P. Rosasco, Build. Environ. 70 (2013) 110–121.
[12] E.D. Carlson et al., Biotechnol. Adv. 30 (2012) 1185–1194.
[13] W.-Q. Liu et al., Biochem. Eng. J. 141 (2019) 182–189.
[14] S.B. Nimse et al., Sensors (Switzerland) 14 (2014) 22208–22229.
[15] D. Guschin et al., Anal. Biochem. 250 (1997) 203–211.
[16] A.W. Peterson, R.J. Heaton, R.M. Georgiadis, Nucleic Acids Res. 29 (2001) 5163–5168.
[17] J. Zlatanova, A. Mirzabekov, in: J.B. Rampal (Ed.), DNA Arrays Methods Protoc. (2001) 17–38.
[18] S.H. Um et al., Nat. Mater. 5 (2006) 797–801.
[19] J.B. Lee et al., Nat. Nanotechnol. 7 (2012) 816–820.
[20] S. Hamada et al., Sci. Robot. 4 (2019) eaaw3512.
[21] S. Hamada, D. Luo, Polym. J. 52 (2020) 891–898.
[22] D. Rosenwasser et al., Int. J. Rapid Manuf. 7 (2018) 203.
[23] N. Park et al., Nat. Mater. 8 (2009) 432–437.
[24] D. Wang et al., J. Am. Chem. Soc. 142 (2020) 10114–10124.
[25] P.R. Buskohl, R.A. Gould, J.T. Butcher, J. Biomech. 45 (2012) 895–902.
[26] F. Caschera, V. Noireaux, Biochimie 99 (2014) 162–168.
[27] F. Caschera, V. Noireaux, Biotechniques 58 (2015) 40–43.
[28] Z.Z. Sun et al., J. Vis. Exp. (2013) e50762.
[29] N. Park et al., Nat. Protoc. 4 (2009) 1759–1770.
[30] S. Preibisch, S. Saalfeld, P. Tomancak, Bioinformatics 25 (2009) 1463–1465.
[31] C.M. Buffinton et al., J. Mech. Behav. Biomed. Mater. 51 (2015) 367–379.
[32] X. Xu et al., Langmuir 29 (2013) 8665–8674.
[33] H. Zhang et al., Nat. Mater. 4 (2005) 787–793.
[34] M. Hua et al., Nature 590 (2021) 594–599.
[35] V. Zhang, D. Rosenwasser, J.E. Sabin, Int. J. Archit. Comput. (2020) 1–21.
[36] A.Y. Chen, C. Zhong, T.K. Lu, ACS Synth Biol 4 (2015) 8–11.
[37] A.S. Khalil, J.J. Collins, Nat. Rev. Genet. 11 (2010) 367–379.
[38] I. Caelen, H. Gao, H. Sigrist, Langmuir 18 (2002) 2463–2467.
[39] P. Bao et al., Lab Chip 19 (2019) 1082–1089.
[40] L. Ahrens et al., Adv. Biosyst. 3 (2019) 1–12.

Please cite this article in press as: Y.A. Pardo et al., Materials Today (2021), https://doi.org/10.1016/j.mattod.2021.10.029